

Spatial analysis of the temperature trends in Serbia during the period 1961–2010

Branislav Bajat · Dragan Blagojević · Milan Kilibarda · Jelena Luković · Ivana Tošić

Received: 16 September 2013 / Accepted: 22 July 2014 / Published online: 1 August 2014
© Springer-Verlag Wien 2014

Abstract The spatial analysis of annual and seasonal temperature trends in Serbia during the period 1961–2010 was carried out using mean monthly data from 64 meteorological stations. Change year detection was achieved using cumulative sum charts. The magnitude of trends was derived from the slopes of linear trends using the least square method. The same formalism of least square method was used to assess the statistical significance of the determined trends. Maps of temperature trends were generated by applying a spatial regression method to visualize the detected tendencies. The obtained results indicate a negative temperature trend for the period before the change year except for winter and a more pronounced positive trend after the change year. Besides being more pronounced, the vast majority of trends after the change year were also clearly statistically significant. Our estimate of the average temperature trend over Serbia is in agreement with those obtained at the global and European scale. Calculated

global autocorrelation statistics (Moran's I) indicate an apparent random spatial pattern of temperature trends across the Serbia for both periods before and after the change year.

1 Introduction

Temperature records show an increase in the global mean temperature between 0.4 °C and 0.8 °C in the last 100 years (IPCC 2007). Recent studies revealed a significant worldwide warming and a general increase in the frequency and persistence of high temperatures (Easterling et al. 2000; Yan et al. 2002; Gay-Garcia et al. 2009). The twentieth century (1901–2000) rise in mean annual temperature (0.8 °C per century) over Europe was found to be slightly greater of worldwide increase (Parry 2000; Luterbacher et al. 2004). Regional climate variations have regional features that often do not match those of the globe as a whole. Greece is differentiated from the rest of Europe in that air temperature shows a slight negative trend over the twentieth century (e.g., Feidas et al. 2004; Nastos et al. 2011).

From the 1990s, the overall warming was found to be even steeper with a trend over the period 1979–2005 of more than 2.5 °C per century (Brohan et al. 2006; Smith and Reynolds 2005). A fast warming was noted in Europe especially from 1979 onward (Klein Tank and Können 2003; Moberg and Jones 2005; Brunet et al. 2006; Della-Marta et al. 2007). In regards to European seasonal warming trends, several studies (Klein Tank and Können 2003; Luterbacher et al. 2004; Smith and Reynolds 2005; IPCC 2007; Ballester et al. 2010) reported the following: (a) a very high increase in temperature in central-northern Europe during winter and (b) an overall fast increase in spring and especially summer season and a frequently not significant (with the exception of northern Europe) and considerable lower increase in autumn.

Many articles have been published dealing with global scale climate changes. However, this article deals with a

B. Bajat · D. Blagojević · M. Kilibarda
Department of Geodesy and Geoinformatics, Faculty of Civil Engineering, University of Belgrade, Bul. kralja Aleksandra 73, 11000 Belgrade, Serbia

B. Bajat
e-mail: bajat@grf.bg.ac.rs

D. Blagojević
e-mail: bdragan@grf.bg.ac.rs

M. Kilibarda
e-mail: kili@grf.bg.ac.rs

J. Luković
Faculty of Geography, University of Belgrade, Studencki trg 3/3, 11000 Belgrade, Serbia
e-mail: jelenal@gef.bg.ac.rs

I. Tošić (✉)
Faculty of Physics, Institute for Meteorology, University of Belgrade, Dobračina 16, 11000 Belgrade, Serbia
e-mail: itosic@ff.bg.ac.rs

regional scale investigation that refers specifically to Serbia. The few published studies on trend analysis of air temperature in the area of Serbia are based either on a single station (Unkašević et al. 2005) or on a limited number of stations (Unkašević and Tošić 2009; Unkašević and Tošić 2013).

The main aim of the present study is to contribute to the knowledge of the behavior of the mean annual and seasonal temperature trends (sign and magnitude) that occurred in Serbia over the last 50 years. In addition, the aims of the paper are as follows:

1. to obtain detailed insight into the spatial distribution of temperature and
2. to analyze the spatial pattern of temperature trends in Serbia using global and local autocorrelation statistics parameters.

The outline of the paper is as follows: after Sect. 1, Sect. 2 describes the study area and data set used in the study. In Sect. 3, the methods are presented. Sect. 4 contains the results and discussion. The conclusions are presented in Sect. 5.

2 Data

2.1 Study area

The study area occupies the territory of Serbia covering an area of 88,361 km², which is nearly 18 % of the Balkan Peninsula. Serbia is located between central and southern Europe and is characterized by a complex topography. The northern part of the country is entirely located within the Pannonian Plain. Several mountain systems cross the country and include the following: (1) the Dinaric Alps stretching through the west and southwestern parts and (2) the Carpathian, Balkan, and Rhodope Mountains occupying the eastern and southeastern regions. The mean altitude of Serbia is 473 m and varies in elevation from 29 m in eastern parts of the country near the borders between Bulgaria and Romania and rises up to 2,656 m on Prokletije Mountain in the south.

Serbia is characterized by three main types of climates: continental, moderate continental, and modified Mediterranean climate. A typical continental climate characterizes the northern parts of the country (Unkašević and Radinović 2000), while the south and southwestern regions are subjected to Mediterranean influences. The Adriatic Sea can significantly affect the inland climate by acting as a source of heat and moisture. However, this influence is modified and is suppressed by the presence of high Dinaric Alps stretching along the coast (Perčec Tadić 2010). Rainfall over Serbia is unevenly distributed reaching an average amount of 739 mm (Bajat et al. 2012). The average temperature over Serbia in the investigated period is 10.4 °C.

2.2 Data set

In this paper, the mean monthly temperatures were analyzed during the period 1961–2010 from 67 meteorological stations provided by the Hydro-Meteorological Service of Serbia. The data is compiled from 31 synoptical stations and 36 climatological stations. The meteorological station network is spatially distributed very well. However, it should be indicated that station networks in mountainous areas are sparse and are of uneven distribution due to the lack of measurements in these areas. A total of 80 % of all meteorological stations are at altitudes of 0–500 m, which comprises 62 % of the territory. A total of 11 % of all stations are placed at altitudes between 500 and 1,000 m, which occupies 27 % of the area. Only 9 % of the stations are at altitudes higher than 1,000 m. The assembled data is quality controlled in terms of the correction of misprints, relocation history, and missing values (WMO 2002). The time series used have been examined previously for homogeneity by Tošić (2005), using the Alexandersson test (Alexandersson and Moberg 1997). As a result, the time series with inhomogeneities from three stations were excluded from further analysis. In order to ensure data quality, we kept 64 meteorological stations with complete series.

The Advanced Spaceborn Thermal Emission and Reflection Radiometer (ASTER) GDEM2 global model (Version 2) of the Earth's surface (<http://asterweb.jpl.nasa.gov/gdem.asp>) was used as data for the digital elevation model. This database is designed for advanced spatial analysis at regional and subregional scale. The ASTER GDEM data are distributed in a GeoTIFF format with a spatial resolution of 30 m and an estimated height accuracy of 17 m at the 95 % confidence level. For the purpose of this study, the initial data were resampled to match the 1-km grid resolution.

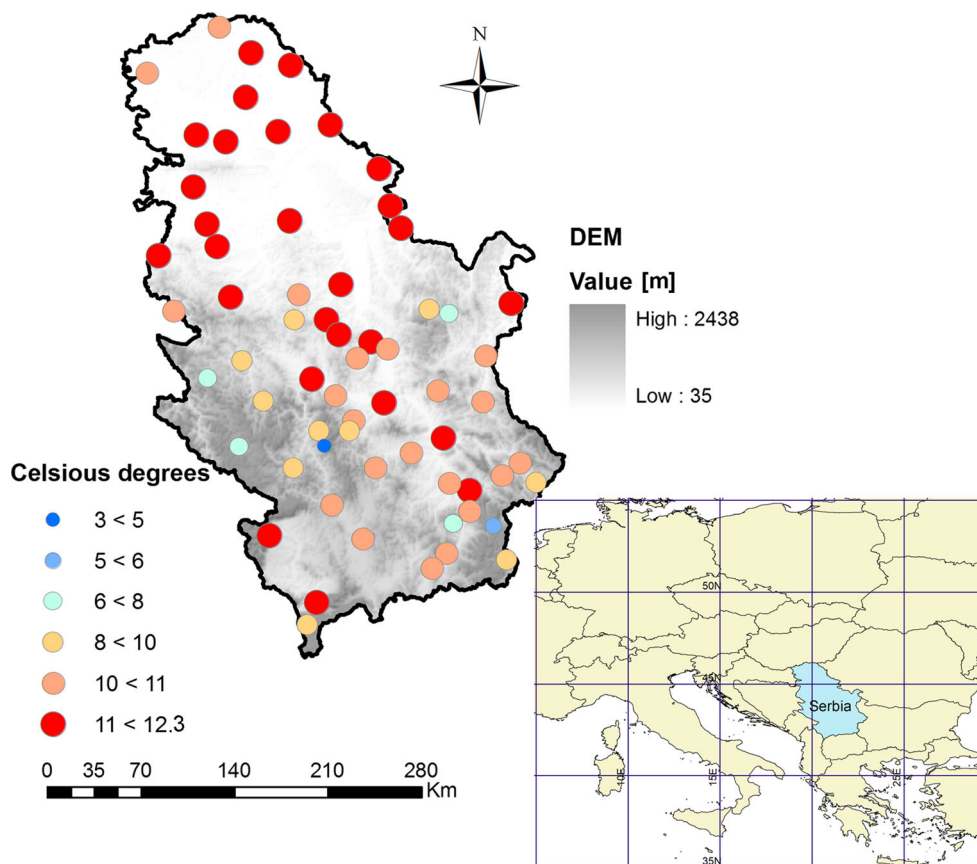
Figure 1 shows the locations of meteorological stations. For each station, monthly values were averaged to obtain the annual and seasonal values.

2.3 Temperatures for the period 1961–2010

As can be seen from Fig. 1, the mean annual temperatures are between 10 and 12 °C in the regions of the lowlands in northern Serbia, the Velika Morava River, and in southwestern Serbia. Mean annual temperatures were below 10 °C at altitudes higher than 600 m in central and southeastern Serbia and were around 6 °C at altitudes above 1,000 m in western Serbia. The lowest mean annual temperatures were around 3 °C at altitudes above 1,500 m.

It was not possible to apply some of the most common interpolation methods in order to make an isotherm map due to the scarce distribution of considered stations over the study area. For that reason, the simple regression model was applied to obtain a map of mean annual temperatures of Serbia for the period of 1961–2010. Climatological regression models

Fig. 1 Locations of stations with associated mean annual temperatures (1961–2010)



usually incorporate longitude, latitude, and terrain heights as explanatory variables in climatological regression models (Gómez et al. 2008). However, due to the small spatial spreading of Serbia (covered area of 88,361 km²), terrain altitudes alone indicate significant influence ($p < 0.001$) in the explanation of mean annual temperatures with a satisfactory coefficient of determination $R^2 = 0.83$:

$$T = 11.973 - 0.0044h \quad (1)$$

where T represents the mean annual temperature in Celsius degrees and h stands for terrain altitude.

Based on the estimated regression model (Eq. 1), the isothermal map could be easily produced in a geographical information system (GIS) environment by using an appropriate digital elevation model (DEM) as an input layer. The majority of spatial data required for environmental modeling are publically available in GIS formats as global data sets. The results of the spatial prediction are produced as a raster GIS layer in the same resolution as the input layer. The map of the mean annual temperatures of Serbia for the period 1961–2010 is shown in Fig. 2.

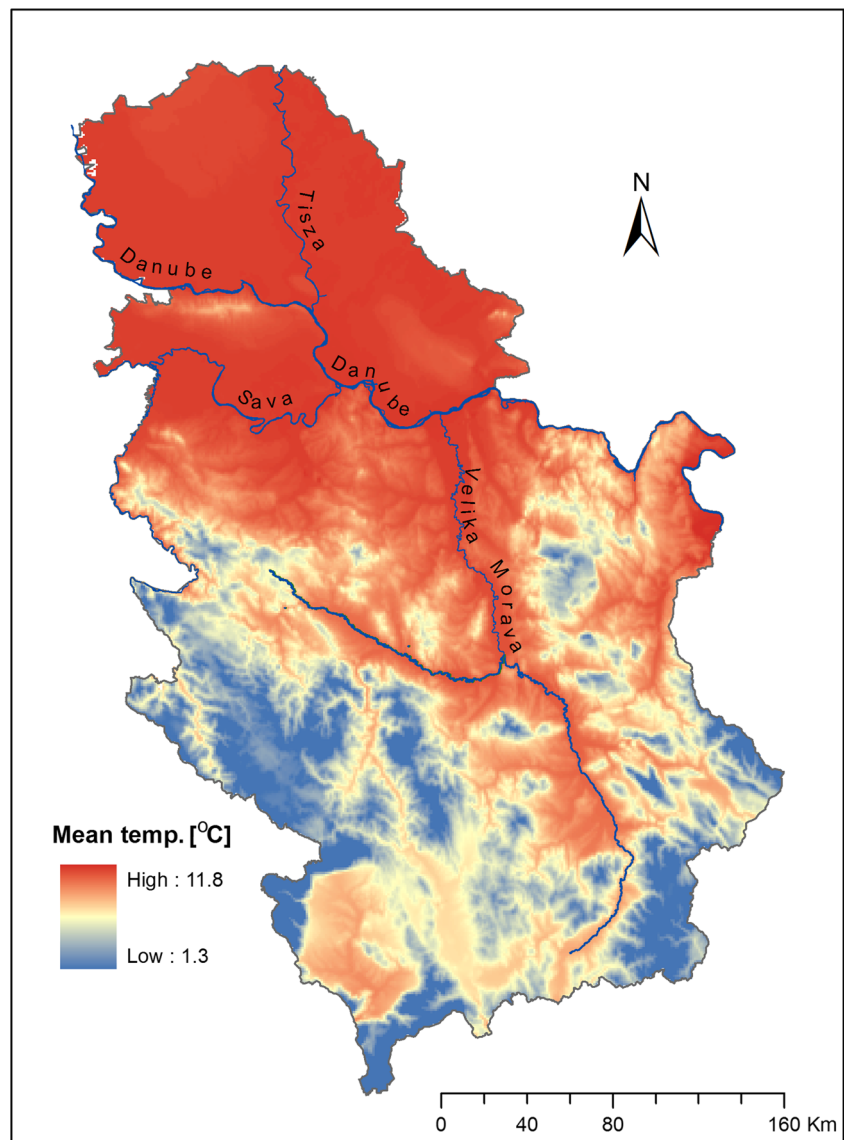
The model's residuals were obtained through the leave one out cross-validation process providing a mean error of ME =

-0.01 °C and root-mean-square error RMSE = 0.70 °C. The finest details in the different temperature range areas are apparent as a result of the use of DEM (Fig. 2).

The temperature map of Serbia for the period 1961–2010 showed that the temperature conditions in the valleys of the Sava, Danube, Tisza, Velika Morava, and Južna Morava Rivers were between 11 and 12 °C. These areas presented the highest mean annual temperatures in the investigated period (Fig. 2). The area with the mean annual air temperature below 10 °C extended generally at altitudes above 600 m. This is in line with conclusions made in previous studies (Ducić and Radovanović 2005) using different methods. However, it is important to add that temperature within the given threshold limits was observed at lower altitudes around the areas of Bor, Žagubica, Dimitrovgrad, Užice, and Priština. Mountainous areas with altitudes above 1,000 m had mean annual temperatures of around 6 °C, while altitudes above 1,500 m averaged around 3 °C.

The morphology and aspect of study regions are also significant factors of temperature conditions in addition to altitude. Circulation processes are more dynamic on steep slopes than in valleys, where the air masses are prolonged. An example which supports the influence of morphology is the coldest part of Serbia—the Pešter plateau. All valleys, and particularly those in higher altitudes, are suitable for cold air

Fig. 2 Map of the mean annual temperatures in Serbia (1961–2010)



masses and frequent temperature inversions. Hence, the lowest temperatures in Serbia were recorded in the Pešter plateau and Sjenica valley in southwestern Serbia.

3 Methods

3.1 Trend determination

The least square (LSQ) method was used to estimate trends in data sets. However, simple visual inspection revealed the presence of changing epochs, i.e., years when the series of mean annual temperatures obviously change their slope for every station. Figure 3 shows the example of station Senta as a typical case that illustrates the presence of a changing year.

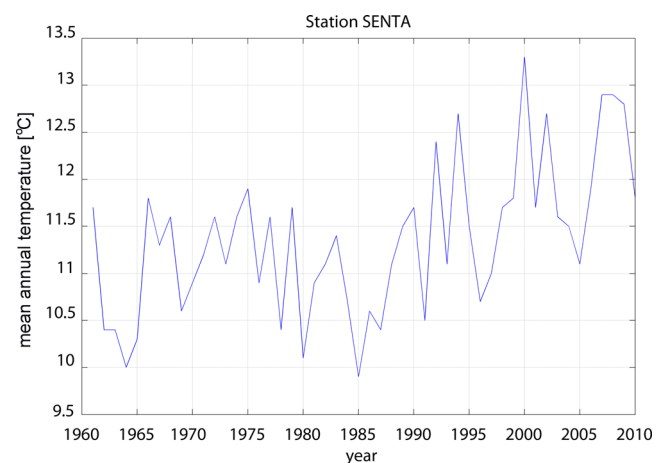


Fig. 3 Example of trend change in mean annual temperature data set for station Senta

For that reason, changing year detection and determination was performed first, before any trend estimation.

Changing year detection and determination was performed by the production of cumulative sums (CUSUM) charts. The CUSUM chart, a graphical method of change year detection, was first introduced by Page (1954). The underlying mathematical principles involved in its construction were elaborated by Ewan (1963), Johnson (1961), and Johnson and Leone (1962). Consider the cumulative sums $s_0, s_1 \dots s_n$ that are calculated from data $x_1 \dots x_n$, which are assumed to be random, as follows ($i=0, 1, \dots, n$):

$$s_i = s_{i-1} - (x_i - \bar{x}) \tag{2}$$

where $s_0=0$ and \bar{x} denote the mean value of data. Plots of CUSUMs s_i against i generates CUSUM charts. If there are no changes in the mean, the CUSUM charts display a steady (flat line) straight path, since the data are random. Otherwise, a segment of the CUSUM chart with an upward slope indicates a period where the values tend to be above average, or a segment with a downward slope indicates a period of time where the values tend to be below average. A sudden change s_{diff} in the slope of the CUSUM occurs with a sudden shift in the average. The magnitude of the sudden change, $|s_{diff}|$, can be estimated from the following:

$$s_{diff} = \max_{i=0,1,\dots,n} s_i - \min_{i=0,1,\dots,n} s_i \tag{3}$$

Efron and Tibshirani (1993) proposed a bootstrap analysis based on the random reordering of the elements of the series with replacement, which can be used to calculate the confidence level as an indication whether a mean shift has occurred. Once a change has been detected, the location of the change needs to be determined. Among others, a natural and simple approach is to use the following expression:

$$s_m = \max_{i=0,1,\dots,n} |s_i| \tag{4}$$

where s_m is the point furthest from 0 in the CUSUM chart. The m point gives the last data point before the change occurred, and the $m+1$ point refers to the first data after the change.

An important precondition for CUSUM charts and changing year detection is to ensure the randomness of data series. If serial correlation exists in data, the series can be prewhitened using lag-1 correlation coefficient r_1 calculated according to the following:

$$r_1 = \frac{\frac{1}{n-1} \sum_{i=1}^{n-1} (x_i - \bar{x})(x_{i+1} - \bar{x})}{\frac{1}{n} \sum_{i=1}^n (x_i - \bar{x})^2} \tag{5}$$

In the case of statistical significant correlation coefficient, the new data set which is free from serial correlation can be constructed as $x_2 - r_1x_1, x_3 - r_1x_2$, etc.

In order to gain some deeper insight into behavior of station temperatures, an LSQ algorithm (Koch 1988) was used for trend determination in data sets of monthly temperature values. At each station, the following model was used:

$$x_i = a + b(t_i - 1961.0) + c \cos 2\pi(t_i - 1961.0) + d \sin 2\pi(t_i - 1961.0) \tag{6}$$

with a being the intercept, b the value of slope (trend), and c and d can be used to calculate the amplitude A of annual periodic signal which is readily visible in series of mean monthly temperatures according to the following:

$$A = \sqrt{c^2 + d^2} \tag{7}$$

Model 6 was used twice for every station: first with data before the changing year, and then with data after the changing year.

3.2 Global and local spatial autocorrelation indices

The global Moran's I and local Getis-Ord G_i^* spatial statistics were used in order to describe spatial autocorrelation globally and to identify different types of clustered spatial patterns of temperature trends.

Spatial autocorrelation of mean annual temperatures in addition to annual and seasonal trends was calculated by Moran's I statistic (O'Sullivan and Unwin 2003):

$$I = \frac{n}{\sum_{i=1}^n (y_i - \bar{y})^2} \frac{\sum_{i=1}^n \sum_{j=1}^n w_{ij} (y_i - \bar{y})(y_j - \bar{y})}{\sum_{i=1}^n \sum_{j=1}^n w_{ij}} \tag{8}$$

where y_i and y_j are the observed values of the considered variable at the locations i and j , \bar{y} is the mean value, and w_{ij} is the spatial weight measure that represents proximity of locations i and location j , often calculated as the inverse of the

distance between point i and point j , and n represents the number of stations.

The value of the Moran's I statistic ranges from near +1 indicating clustering of the y values to near -1 indicating dispersed pattern of the y values. In order to evaluate the statistical significance of the Moran's I statistic, a standardized Z score value is calculated as the following:

$$Z_I = \frac{I - E[I]}{\sqrt{V[I]}} \tag{9}$$

where $E[I]$ is the expected value of I , assuming random spatial pattern:

$$E[I] = \frac{-1}{(n-1)} \tag{10}$$

and $V[I]$ represents the variance of I .

In the global Moran's I statistic, the results of the analysis are always interpreted within the context of its null hypothesis which states that the variable being analyzed is randomly distributed among the stations in our study area, or better said, the spatial processes promoting the observed pattern of values are random chance. The results of Moran's I statistic with significant p values and positive Z scores indicate spatially clustered data sets. However, at the same time, negative Z scores depict that spatial pattern is more spatially dispersed.

Moran's I is the global statistic index that summarizes the values of autocorrelation over the entire study region. In the case of statistically immanent spatial autocorrelation, it is necessary to calculate local autocorrelation indices like *Getis-Ord Gi** statistics in order to indicate the level of spatial autocorrelation at the local scale (Ord and Getis 1995):

$$G_i^* = \frac{\sum_{j=1}^N w_{ij} y_j - \bar{y} \sum_{j=1}^N w_{ij}}{S \sqrt{\frac{N \sum_{j=1}^N w_{ij}^2 - \left(\sum_{j=1}^N w_{ij} \right)^2}{N-1}}} \tag{11}$$

where w_{ij} is the element in adjacency as stated in Eq. 8 and S is given as the following:

$$S = \sqrt{\frac{\sum_{j=1}^N x_j^2}{N} - (\bar{x})^2} \tag{12}$$

This local indicator represents a disaggregated measure of autocorrelation that depicts the extent to which a particular observed station is similar to or different from neighboring

stations or the extent to which the station is surrounded by a cluster of high or low values. *Getis-Ord Gi** statistics is used to detect possible nonstationarity of the data, i.e., clustering pattern in specific subregions.

Hot Spot Analysis (Lee and Wong 2005) incorporating *Getis-Ord Gi** statistics provides more insight into how the stations with high and low trends are clustered, indicating the extent to which each sample is surrounded by similar high or low values. The best way to interpret the *Getis-Ord Gi** statistic is in the context of the standardized Z score values. A high positive Z score of G_i statistics appears when the spatial clustering is formed by similar but high values; the larger the Z score is, the more intense the clustering of high values. The Z score will tend to be highly negative if the spatial clustering is formed by low values, whereby the smaller the Z score is, the more intense the clustering of low values. A Z score around 0 indicates no apparent spatial association pattern.

3.3 Thematic mapping by plotGoogleMaps

To gain better insight into the results obtained as thematic maps, we used a recently developed package in the R language environment, plotGoogleMaps, based on Asynchronous JavaScript and XML (AJAX) and Google Maps Application Programming Interface (API) service that produces HyperText Markup Language (HTML) file map mashups (Web maps), with high-resolution Google Map as a base map. The tool

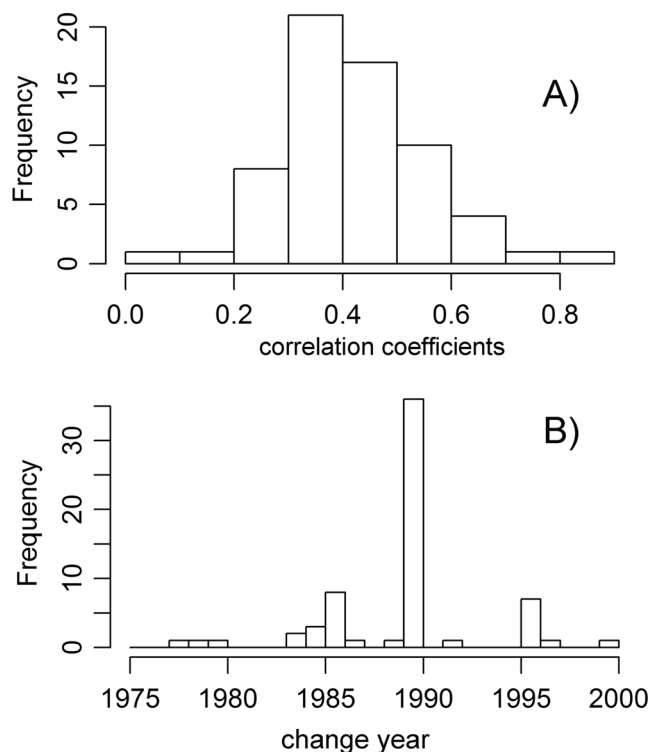


Fig. 4 Histograms of **a** lag-1 correlation coefficients and **b** change epochs

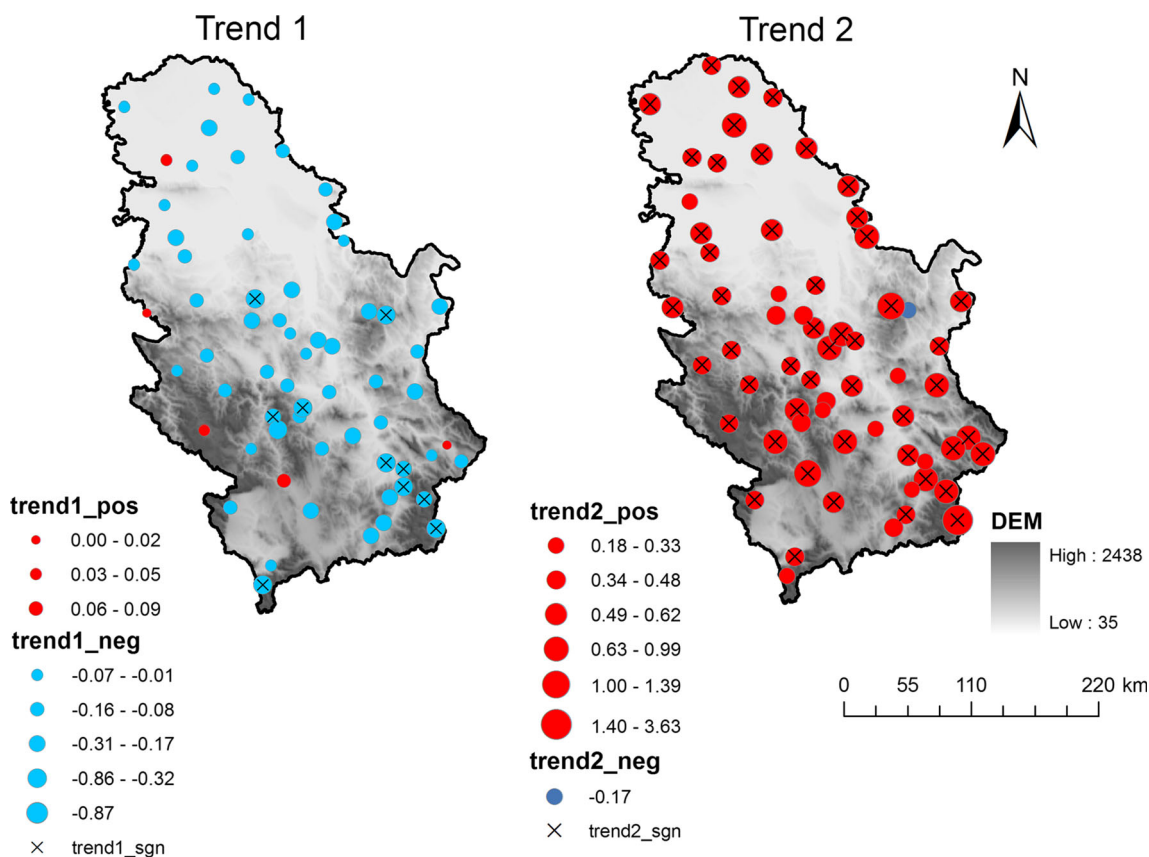


Fig. 5 Spatial distribution of the annual temperature trend coefficients over Serbia from 1961 to 2010, before the change year (*left*) and after the change year (*right*). The bubbles with \times signs inside the circles represent

stations with significant positive and negative trends at significance level of 5 %. Legend units $^{\circ}\text{C}/\text{decade}$

plotGoogleMaps is developed in the open source R software language, and it is designed for the automatic creation of Web maps that are formed through a combination of users' data and Google Maps layers (Kilibarda and Bajat 2012).

When compared to other classical graphic device environment, plotGoogleMaps offers more advantages that include high quality of background Google layers for better abstractions of geographical reality, spatial data exploration functionality, and map interactivity (navigation control, pan, zoom, attribute info windows, etc). All produced maps are available in HTML format at the Web page URL: http://www.grf.bg.ac.rs/~bajat/temperature/Temp_trends.htm.

4 Results and discussion

4.1 Temperature trends

The first step in the analysis of the temperature time series was the identification of possible change years, i.e., time epochs with trend change for every station. The analysis was performed on a series of mean annual and seasonal station

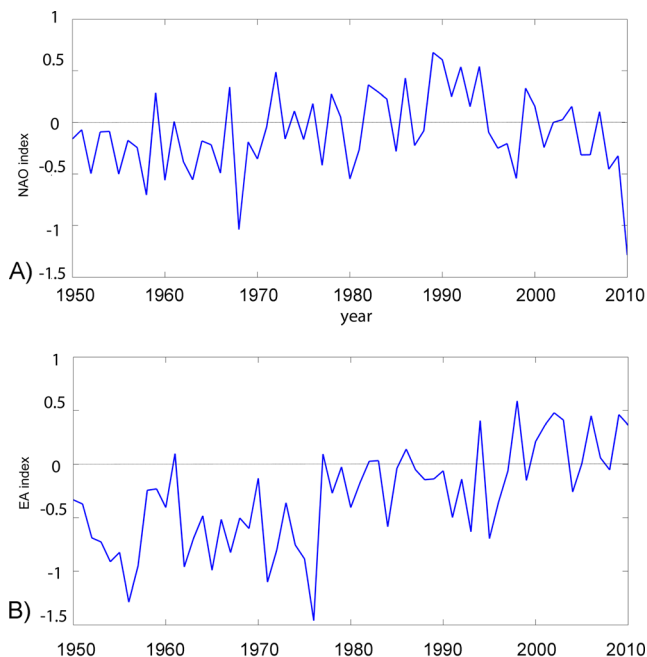


Fig. 6 The annual time series of the **a** NAO index and **b** EA index during the period 1950–2010

temperatures. Prewhitened data sets were obtained by the calculation of a lag-1 correlation coefficient according to Eq. 5. A histogram of correlation coefficients is shown in Fig. 4a. It can be seen that there is an exclusively positive serial correlation present in temperature data with the majority of correlation coefficients being in the range 0.2–0.6. Following Salas et al. (1980), the two-sided probability limits of correlation coefficient for 95 % significance level can be calculated as follows:

$$r_k(95\%) = \frac{-1 \pm 1.96\sqrt{N-k-1}}{N-k} \quad (13)$$

where N denotes the sample size, and k is the lag. For $N=50$ and $k=1$, the above formula yields probability limits of -0.30 and $+0.26$, thus confirming statistical significance for 91 % of correlation coefficients. Nevertheless, every data set was prewhitened independently of significance of the lag-1 correlation coefficient.

CUSUM charts were produced for the detection of change years at every station, and the years representing the trend

change were determined according to Eq. 4. A histogram of these years is shown in Fig. 4b. The changes in the temperatures have occurred approximately from the end of the 1970s through the end of the 1990s. The most pronounced change year is 1989, which together with epochs 1985 and 1995 contains about 80 % of all years obtained by CUSUM charts. Change years were then used to divide every station's temperature series into two time intervals. The functional model 6 was considered adequate for these time intervals.

By applying the LSQ method, an analysis of the mean monthly temperature series reveals a cooling period first, followed by a change point in 1989 (at 35 of 64 stations), and then a warming period. In Europe, a cooling period followed by a warming period starting in the mid-1970s has been found (Balling et al. 1998; Klein Tank et al. 2002). Gurevich et al. (2011) found that the change in the temperatures in Israel has occurred approximately between the mid-1980s and the mid-1990s. Toreti and Desiato (2008), by applying the sloped steps model in the analysis of the annual mean temperature anomaly series in Italy, revealed first a cooling period, a change point in 1981, and then a warming period.

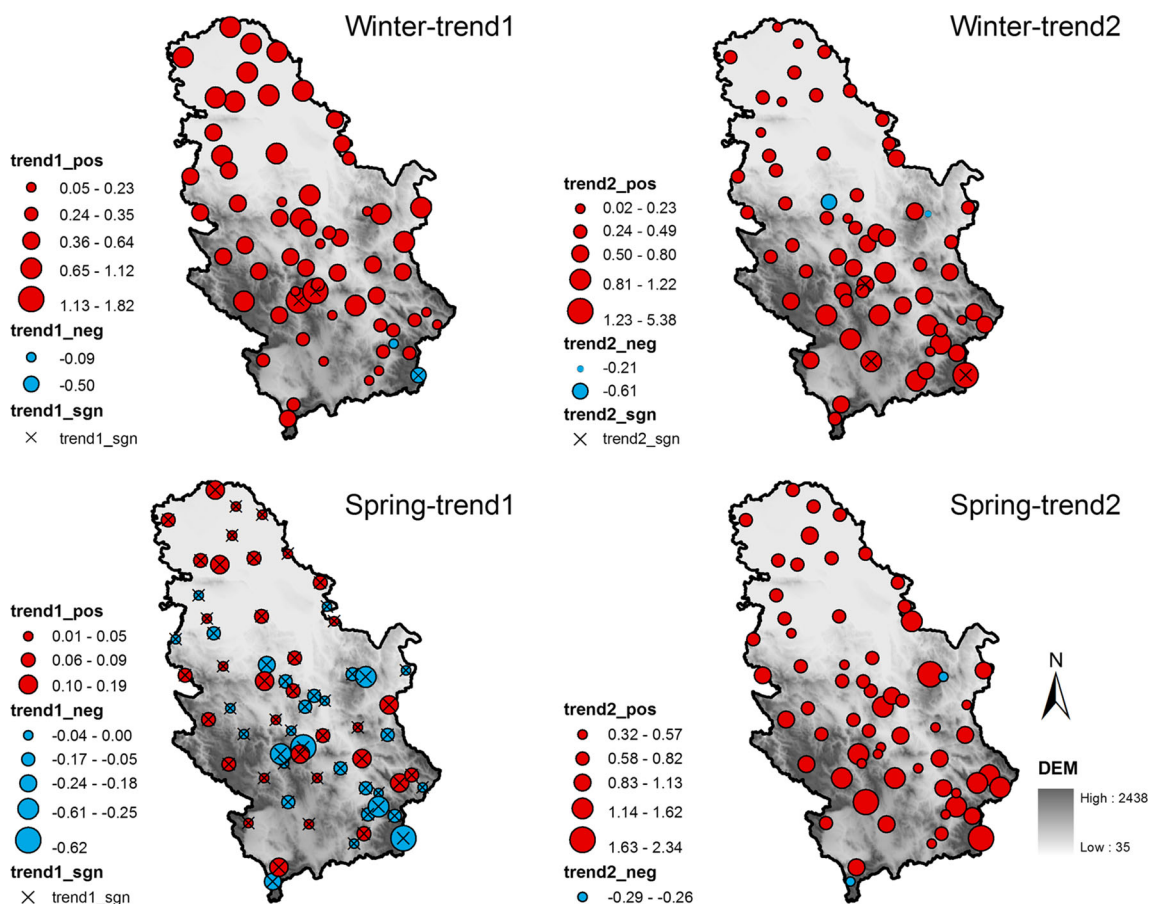


Fig. 7 Spatial distribution of temperature trend coefficients over Serbia for winter (top) and spring (bottom) before the change year (left) and after the change year (right). The bubbles with \times signs inside the circles

represent stations with significant positive and negative trends at significance level of 5 %. Legend units $^{\circ}\text{C}/\text{decade}$

In the period before the change year, a negative trend with a slope of -0.01 to -0.87 °C/decade and a significance level greater than 95 % has been estimated at the ten stations (Fig. 5 left). A slightly positive trend is observed at only six stations. The second period, which is the period after the change year, shows a positive trend from 0.18 to 3.63 °C/decade with a significance level greater than 95 % at almost all stations (Fig. 5 right). A negative trend is recorded at only one station.

These results may be compared with those of the study on European mean annual temperature. Brunet et al. (2005) reported a negative trend of 0.29 °C/decade in a study of mean annual temperature series over Spain during the period of 1948–1973. They also report a change to a positive trend of 0.54 °C/decade from 1973 to 2003. The negative trend that Klein Tank and Können (2003) estimated in -0.04 °C/decade over the period 1946–1999 showed a reversal pattern in regard to the 1976–1999 period. Our results for the second time period are in accordance with what has been reported by Unkašević et al. (2005), who have noted an increase of about 1.3 °C/decade for Belgrade (Serbia) during the period 1975–2003.

Several authors have associated increase in the mean annual temperature with the positive phase of the North Atlantic Oscillation (NAO) since this pattern is recognized as the main mode of climate variability in the extratropical Northern Hemisphere (e.g., Hurrell 1995; Sun et al. 2009; del Río et al. 2011). The East Atlantic (EA) pattern is also being recognized as a pattern that characterizes climate variability in the Northern Hemisphere. The anomaly centers of the EA pattern are displaced southeastward to the approximate nodal lines of the NAO pattern (Barnston and Livezey 1987). The NAO and EA patterns were analyzed through the NAO index (NAOI) and EA index (EAI), that are presented in Fig. 6. From Fig. 6a, it can be seen that a positive phase of the NAOI prevailed from the beginning of the 1980s to the beginning of the 2000s. A positive phase of the EAI prevailed after the mid of 1990s (Fig. 6b). Hence, it can be concluded that the warming in Serbia (after the change year) is influenced by both NAO and EA patterns.

On a seasonal timescale, temperature increase from 0.02 to 1.82 °C/decade is observed all over the Serbian territory during the winter season in both periods, statistically

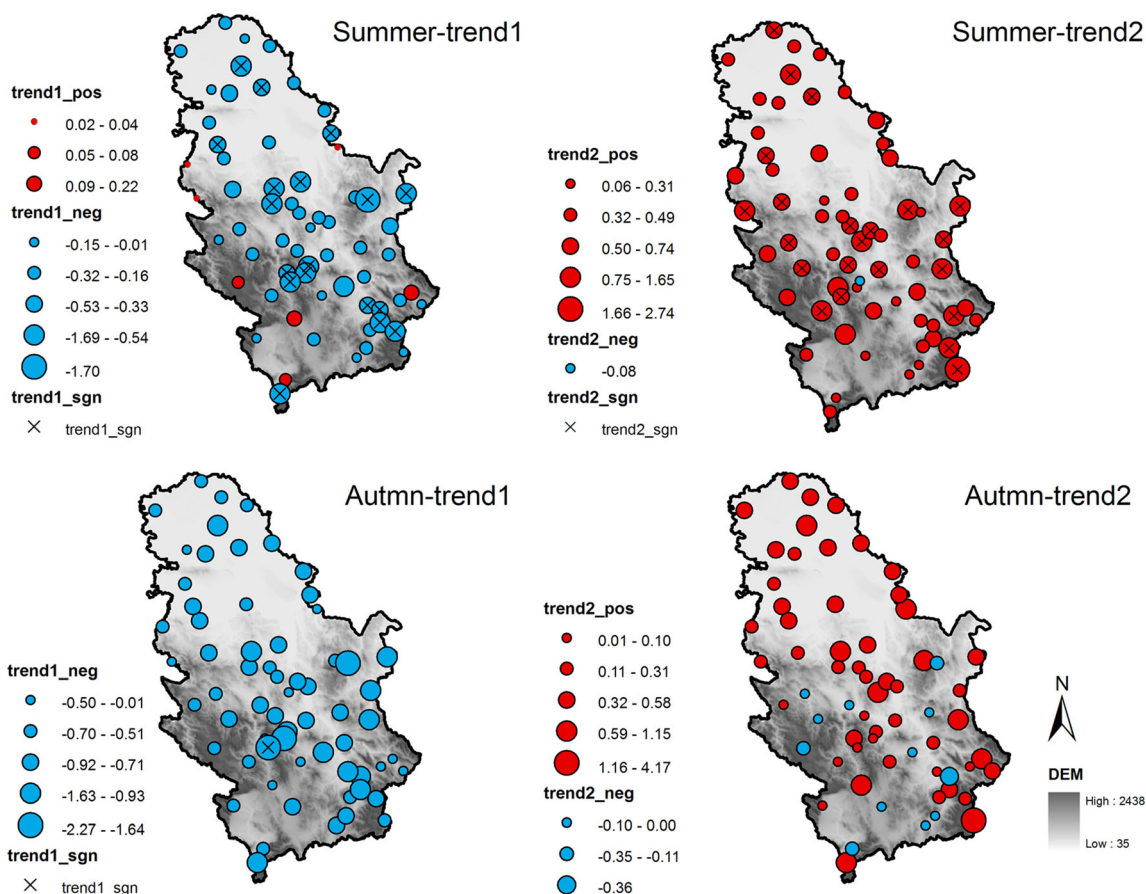


Fig. 8 Spatial distribution of temperature trend coefficients over Serbia for summer (top) and autumn (bottom) before the change year (left) and after the change year (right). The bubbles with \times sign inside the circles

represent stations with significant positive and negative trends at significance level of 5 %. Legend units °C/decade

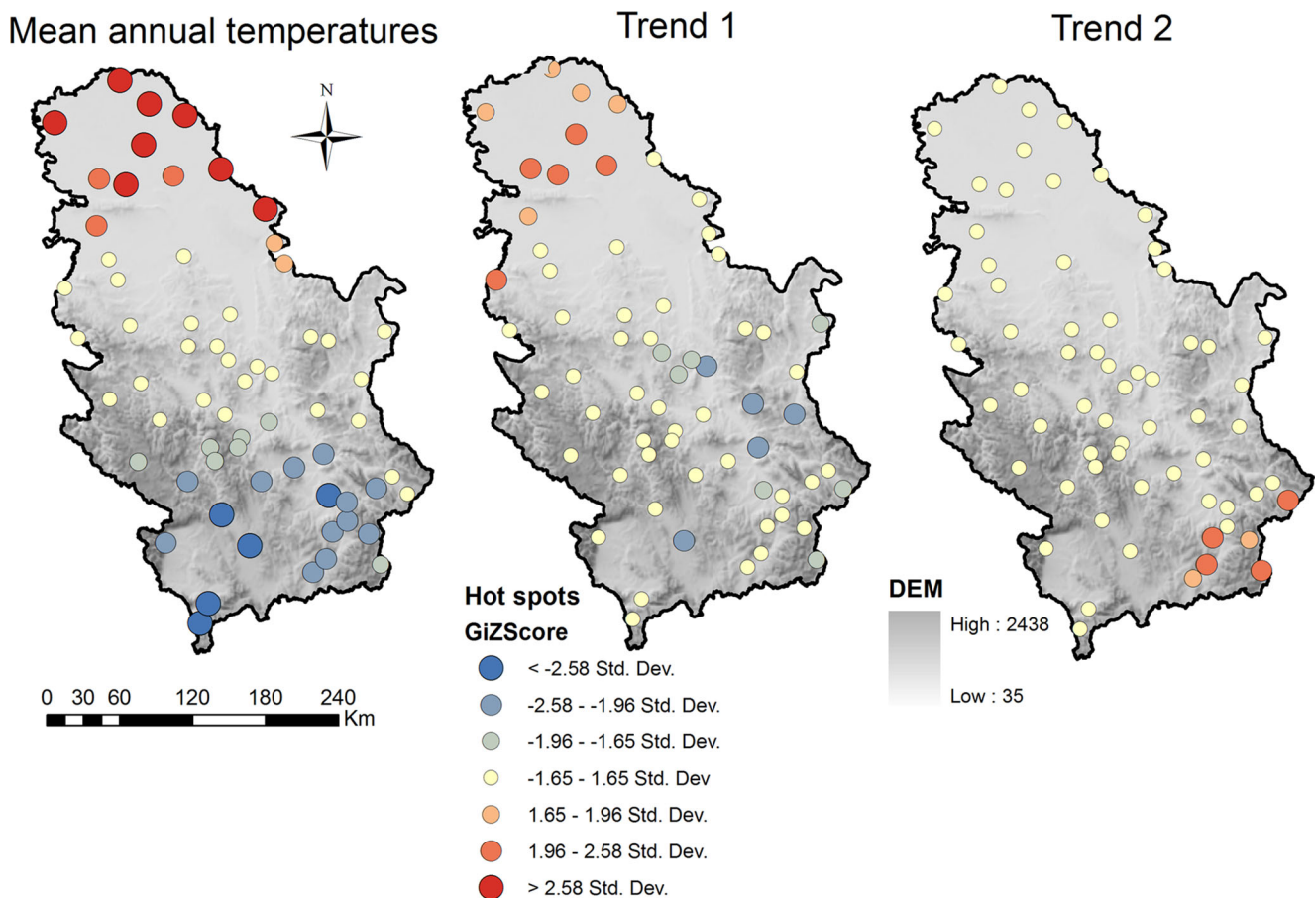


Fig. 9 Mapped Z scores of Gi statistics of calculated mean annual temperatures and trends

significant at two stations (Fig. 7). Only exception is a temperature decrease registered at two stations in both periods. During the spring season (Fig. 7), there is no particular spatial pattern of positive and negative trends characterizing first period. A slight nonsignificant increase from 0.32 to 2.34 °C/decade, however, is noticed in the second period.

Summer season (Fig. 8) revealed negative trend from -0.01 to -1.70 °C/decade in the first period, significant at 18 stations. A positive trend is registered after the change year with values between 0.06 and 2.74 °C/decade, statistically significant at 22 stations.

Results for autumn (Fig. 8) are similar for those calculated for summer, with negative values from -0.01 to -2.27 °C/decade before the change year, but significant at only one station. A slight temperature increase prevailed in Serbia during the second period.

Brunet et al. (2007) found a strong rise in Spanish temperatures since 1973 (on an annual basis) associated with greater increases for spring and summer temperatures compared to those for winter and autumn. Philandras et al. (2008), analyzing annual and seasonal temperatures from 20 meteorological stations in Greece, noted a cooling trend till the middle of the decade of 1970, when the trend reversed to heating. Only

exception existed in spring when a slight heating trend in the northern region of Greece is noted.

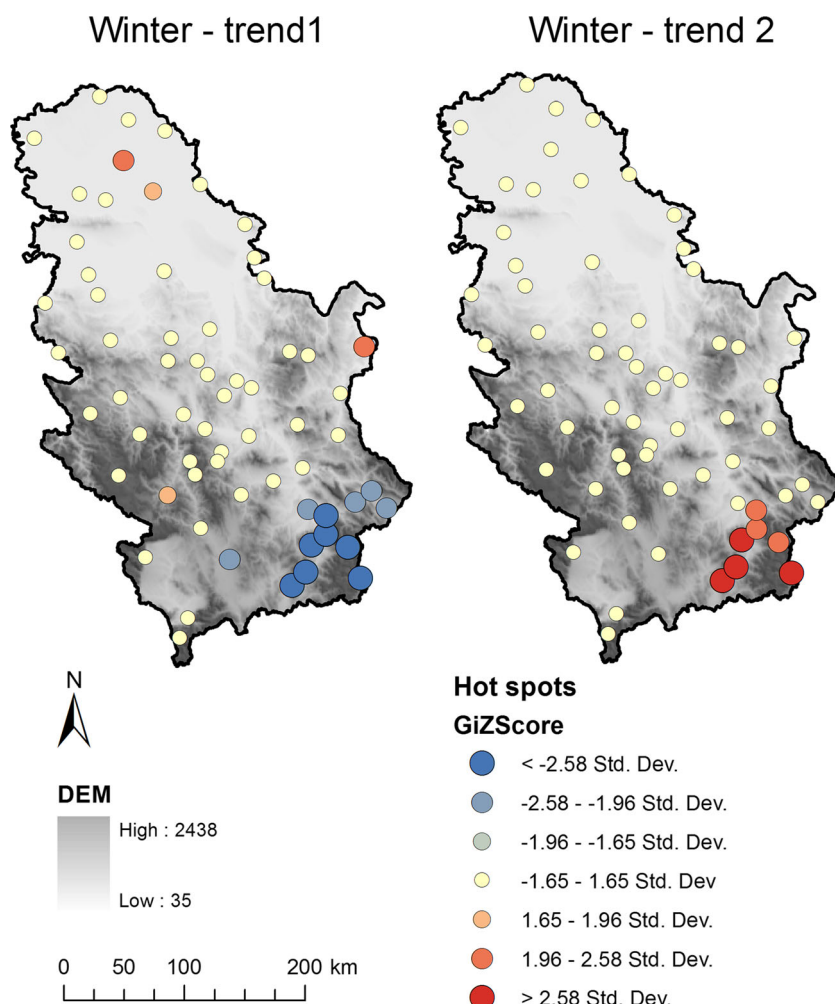
4.2 Spatial autocorrelation statistics

The calculated value of mean annual temperatures (1961–2010) for *Moran's index* $I=0.052$ (Z score= 4.342 , $p<0.001$) indicates statistically significant clustering but low spatial autocorrelation for the overall pattern of observations. Almost the same result was obtained for *trend 1*, $I=0.052$ (Z score= 4.342 , $p<0.001$). At the same time, *Moran's index* $I=0.0001$ (Z score= 1.342 , $p=0.1$) for *trend 2* confirms the null hypothesis “there is no spatial clustering of the values associated with the stations in the study area.”

In order to gain better insight into how the stations with high and low levels of mean annual temperatures and trends are clustered, Hot Spot Analysis by calculating Getis-Ord Gi statistics was performed despite the low values of global spatial autocorrelation indices (Fig. 9).

The red-colored spots (hot spot) for mean annual temperatures point out statistically significant clustering of high values in the northern part of Serbia, while negative Z score values indicate clustering of low temperature values (blue

Fig. 10 Mapped Z scores of Gi statistics of calculated winter season temperature trends



colored) in the southern part of the country. Such clustering can be attributed to effects of orography. For example, northern Serbia is located in the Pannonian Plain. Hence, high values are expected due to flat and relatively uniform terrain of this region. Local Gi Z score values approve results of global Moran's I for both of the trends. A prevailing number of yellow spots (stations with low Z score and high p values) indicate no apparent spatial clustering of either low or high trend values in both cases.

The values of Moran's index for seasonal temperature trends indicate moderate clustered spatial patterns with high statistical significance only during the winter season for both periods, specifically for *trend 1* $I=0.050$ (Z score=4.124, $p<0.001$) and *trend 2* $I=0.044$ (Z score=5.836, $p<0.001$). The obtained global Moran's I statistic for all other seasons indicate that observed spatial pattern of trends could be the result of random spatial processes.

Figure 10 depicts clustering of low trend values (blue colored) for the winter season in the period before change year and high trend values (red colored) in the period after the

change year in the southeastern part of the country. Analyzing seasonal climate indices based on daily temperatures in Serbia (1950–2009), Knežević et al. (2014) have shown positive winter trend over the most of the Serbia with the exception of southeastern parts of the country which have revealed negative trends. Significant winter spatial clustering shown in Fig. 10 may indicate this suggesting also trend change over the examined period.

5 Conclusions

The mean annual and seasonal temperature series from 64 meteorological stations were used in order to calculate trends in Serbia from 1961 to 2010. A series of CUSUM charts were produced for every station in order to detect change years. The results of the change year analysis in the annual and seasonal temperatures showed that these years could be detected for all series. The CUSUM charts produced by prewhitened

temperature series indicate a change year in 1989 at the majority of stations. The two time intervals, before and after the change year, were then studied separately. The LSQ model estimated an average temperature decrease of -0.01 to -0.87 °C/decade before the change year, followed by an increase of 0.18 to 3.62 °C/decade after the change year. Based on results of statistical testing within the LSQ formalism, it can be said that significant warming was found in almost the whole of Serbia during the last two decades.

Our estimate of the average temperature trend over Serbia is in agreement with those obtained at the global and European scale, although the average change year for Serbia seems to be shifted by a few years. Most of the annual temperature series analyzed here confirm a warming trend beginning at the end of the 1970s, which has already been found from mean temperature time series analysis at both European (Klein Tank and Können 2003) and Serbian scale (Unkašević et al. 2005). By analyzing the time series of the NAO and EA indexes, we concluded that the warming in Serbia (after the change year) is influenced not only by the NAO, but with the EA pattern too.

It was found that the summer season has been the season with the largest contribution to annual trends. A significant positive trend at the 5 % level of significance is registered after the change year at 22 stations.

As is noted in the results above, cluster analysis of mean annual temperatures (1961–2010) depicted that they are weakly clustered with high mean annual temperature values in the northern part of Serbia and low values in the southern part. The similar spatial pattern refers to spatial distribution of the annual temperature trend values before the change year, while the trends after the change year indicate no apparent spatial clustering pattern. The moderate clustered spatial pattern of temperature trends is presented only during the winter season.

As a future work, the authors plan to investigate maximum and minimum temperature trends in Serbia in order to comprehend the regional patterns of extreme events.

Acknowledgments We greatly acknowledge data provided by the Republic Hydrometeorological Service of Serbia. NAO and EA Index values are downloaded from ftp://ftp.cpc.ncep.noaa.gov/wd52dg/data/indices/ea_index.tim. This study was supported by the Serbian Ministry of Education, Science and Technological Development, under Grants No. III 43007, III 47014, TR 36035, TR 36020, and 176013.

References

- Alexandersson H, Moberg A (1997) Homogenization of Swedish temperature data. Part I: homogeneity test for linear trends. *Int J Climatol* 17:25–34
- Bajat B, Pejović M, Luković J, Manojlović P, Ducić V, Mustafić S (2012) Mapping average annual precipitation in Serbia (1961–1990) by using regression kriging. *Theor Appl Climatol* 112:1–13
- Ballester J, Rodó X, Giorgi F (2010) Future changes in central Europe heat waves expected to mostly follow summer mean warming. *Clim Dyn* 35:1191–1205
- Balling RC, Michaels PJ, Knappenberger PC (1998) Analysis of winter and summer warming rates in gridded temperature timeseries. *Clim Res* 9:175–181
- Barnston AG, Livezey RE (1987) Classification, seasonality and persistence of low-frequency atmospheric circulation patterns. *Mon Wea Rev* 115:1083–1126
- Brohan P, Kennedy JJ, Harris I, Tett SFB, Jones PD (2006) Uncertainty estimates in regional and global observed temperature changes: a new dataset from 1850. *J Geophys Res* 111, D12106. doi:10.1029/2005JD006548
- Brunet M, Sigró J, Saladié O, Aguilar E, Jones PD, Moberg A, Walther A, López D (2005) Spatial patterns of long-term Spanish temperature change. *Geophys Res Abs* 7:04007
- Brunet M, Saladié O, Jones PD, Sigró J, Aguilar E, Moberg A, Lister D, Walther A, Lopez D, Almaraz C (2006) The development of a new dataset of Spanish daily adjusted temperature series (SDATS) (1850–2003). *Int J Climatol* 26:1777–1802
- Brunet M, Jones PD, Sigró J, Saladié O, Aguilar E, Moberg A, Della-Marta PM, Lister D, Walther A, López D (2007) Temporal and spatial temperature variability and change over Spain during 1850–2005. *J Geophys Res* 112, D12117. doi:10.1029/2006JD008249
- del Río S, Herrero L, Pinto-Gomes C, Penas A (2011) Spatial analysis of mean temperature trends in Spain over the period 1961–2006. *Global Planet Change* 78:65–75
- Della-Marta PM, Haylock MR, Luterbacher J, Wanner H (2007) Doubled length of western European summer heat waves since 1880. *J Geophys Res* 112, D15103. doi:10.1029/2007JD008510
- Ducić V, Radovanović M (2005) Klima Srbije (climate of Serbia). *Zavod za udžbenike i nastavna sredstva, Belgrade*, p 212 (in Serbian)
- Easterling DR, Meehl GA, Parmesan C, Changnon SA, Karl TR, Mearns LO (2000) Climate extremes: observations, modeling and impacts. *Science* 289:2068–2074
- Efron B, Tibshirani R (1993) *An introduction to the bootstrap*. Chapman & Hall, New York
- Ewan WD (1963) When and how to use CUSUM charts. *Technometrics* 5:1–32
- Feidas H, Makrogiannis T, Bora-Senta E (2004) Trend analysis of air temperature time series in Greece and their relationship with circulation using surface and satellite data: 1955–2001. *Theor Appl Climatol* 79:185–208
- Gay-García C, Estrada F, Sanchez A (2009) Global and hemispheric temperatures revisited. *Clim Change* 94:333–349
- Gómez JD, Etchevers JD, Monterroso AI, Gay C, Campo J, Martínez M (2008) Spatial estimation of mean temperature and precipitation in areas of scarce meteorological information. *Atmósfera* 21:35–56
- Gurevich G, Hadad Y, Ofir A, Ohayon B (2011) Statistical analysis of temperature changes in Israel: an application of change point detection and estimation techniques. *Glob Nest J* 13:215–228
- Hurrell JW (1995) Decadal trends in the North-Atlantic Oscillation—regional temperatures and precipitation. *Science* 269:676–679
- Intergovernmental Panel on Climate Change (IPCC) (2007) *Climate change. The physical science basis*. In: Solomon S, Qin D, Manning M et al (eds) *Contribution of Working Group I to the Fourth Assessment Report of the Intergovernmental Panel on Climate Change*. Cambridge University Press, Cambridge
- Johnson NL (1961) A simple theoretical approach to cumulative sum control charts. *J Am Stat Ass* 56:83–92
- Johnson NL, Leone FC (1962) Cumulative sum control charts—mathematical principles applied to their construction and use. *Ind Qual Control* 18:15–21
- Kilibarda M, Bajat B (2012) PlotGoogleMaps: the R-based web-mapping tool for thematic spatial data. *Geomatica* 66:37–49

- Klein Tank AMG, Können GP (2003) Trends in indices of daily temperature and precipitation extremes in Europe, 1946–99. *J Climate* 16: 3665–3680
- Klein Tank AMG, Wijngaard JB, Können GP et al (2002) Daily dataset of 20th-century surface air temperature and precipitation series for the European Climate Assessment. *Int J Climatol* 22:1441–1453
- Knežević S, Tošić I, Unkašević M, Pejanović G (2014) The influence of the East Atlantic Oscillation to climate indices based on the daily minimum temperatures in Serbia. *Theor Appl Climatol* 116:435–446
- Koch KR (1988) Parameter estimation and hypothesis testing in linear models. Springer Verlag, Berlin
- Lee J, Wong DWS (2005) Statistical analysis of geographic information with ArcView GIS and ArcGIS. Wiley, New York, p 446
- Luterbacher J, Dietrich D, Xoplaki E, Grosjean M, Wanner H (2004) European seasonal and annual temperature variability, trends and extremes since 1500. *Science* 303:1499–1503
- Moberg A, Jones PD (2005) Trends in indices for extremes in daily temperature and precipitation in central and western Europe, 1901–99. *Int J Climatol* 25:1149–1171
- Nastos PT, Philandras CM, Founda D, Zerefos CS (2011) Air temperature trends related to changes in atmospheric circulation in the wider area of Greece. *Int J Remote Sens* 32:737–750
- O’Sullivan D, Unwin D (2003) Geographical information analysis. Wiley, New Jersey, p 436
- Ord JK, Getis A (1995) Local spatial autocorrelation statistics: distributional issues and an application. *Geogr Anal* 27:286–306
- Page ES (1954) Continuous inspection schemes. *Biometrika* 41:100–115
- Parry ML (ed) (2000) Assessment of potential effects and adaptations for climate change in Europe: summary and conclusions. Jackson Environment Institute, University of East Anglia, Norwich, 320 pp
- Perčec Tadić M (2010) Gridded Croatian climatology for 1961–1990. *Theor Appl Climatol* 102:87–103
- Philandras CM, Nastos PT, Repapis CC (2008) Air temperature variability and trends over Greece. *Global Nest Journal* 10:273–285
- Salas JD, Delleur JW, Yevjevich VM, Lane WL (1980) Applied modeling of hydrologic time series: Littleton. Water Research Publications, Colorado
- Smith TM, Reynolds RW (2005) A global merged land and sea surface temperature reconstruction based on historical observations (1880–1997). *J Climate* 18:2021–2036
- Sun JQ, Wang HJ, Yuan W (2009) Role of the tropical Atlantic sea surface temperature in the decadal change of the summer North Atlantic Oscillation. *J Geophys Res* 114, D20110
- Toreti A, Desiato F (2008) Temperature trend over Italy from 1961 to 2004. *Theor Appl Climatol* 91:51–58
- Tošić I (2005) Analysis of temperature and precipitation time series. Ph.D. thesis, Faculty of Physics, University of Belgrade, Belgrade, 164 pp (in Serbian)
- Unkašević M, Radinović Đ (2000) Statistical analysis of daily maximum and monthly precipitation at Belgrade. *Theor Appl Climatol* 66: 241–249
- Unkašević M, Tošić I (2009) An analysis of heat waves in Serbia. *Global Planet Change* 65:17–26
- Unkašević M, Tošić I (2013) Trends in temperature indices over Serbia: relationships to large-scale circulation patterns. *Int J Climatol* 33: 3152–3161
- Unkašević M, Vujović D, Tošić I (2005) Trends in extreme summer temperatures at Belgrade. *Theor Appl Climatol* 82:9–205
- World Meteorological Organization (WMO) (2002) Technical document 1125, GCOS-76. Geneva, Switzerland
- Yan Z, Jones PD, Davies TD, Moberg A, Bergström H, Camuffo D, Coche C, Maugeri M, Demarée GR, Verhoeve T, Thoen E, Barriendos M, Rodríguez R, Martín-Vide J, Yang C (2002) Trends of extreme temperature in Europe and China based on daily observation. *Clim Change* 53:355–392